Physica B 404 (2009) 1332–1335

Contents lists available at ScienceDirect

Physica B

journal homepage: www.elsevier.com/locate/physb

Effect of Schottky barrier on the transport property in perovskite oxide heterostructures

Peng Han [a,b], Hui-bin Lu [a], Kui-juan Jin [a,*], Jin-Feng Jia [b], J. Qiu [a], Chun-lian Hu [a], Leng Liao [a]

[a] Beijing National Laboratory for Condensed Matter Physics, Institute of Physics, Chinese Academy of Sciences, Beijing 100190, China
[b] Department of Physics, Tsinghua University, Beijing 100084, China

ARTICLE INFO

Article history:
Received 15 August 2008
Accepted 13 December 2008

PACS:
73.40.Lq
77.84.Dy
72.20.−i

Keywords:
Self-consistent calculation
Electron-transport
Oxides
Heterostructures

ABSTRACT

The transport processes in the heterostructures of $La_{0.7}Sr_{0.3}MnO_3/BiFeO_3$ and $La_{0.9}Sr_{0.1}MnO_3/SrNb_{0.01}Ti_{0.99}O_3$ have been studied theoretically by taking into account the effect of Schottky barrier formed at the contact of the electrode. By comparing with the experimental data, it is found that the physical origin for the symmetry of the measured *I–V* curves in the heterostructures of $La_{0.7}Sr_{0.3}MnO_3/BiFeO_3$ can be attributed to the effect of the Schottky contact diodes. It is also found that the influence of Schottky barrier on the transport properties of $La_{0.9}Sr_{0.1}MnO_3/SrNb_{0.01}Ti_{0.99}O_3$ heterostructures increases with the increased temperature and decreases with the increased doping density of $SrNb_{0.01}Ti_{0.99}O_3$ layer at temperature above the Curie temperature of $La_{0.9}Sr_{0.1}MnO_3$ based on our calculation.

1. Introduction

The perovskite oxide heterostructures such as all-oxide and oxide-silicon p–*i*–n diodes [1], p–n junctions [2–5], and Schottky junctions [6,7] have been the areas of active research for their potential application in the next generation of integrated circuit. Besides the vigorous research efforts from the experimental aspect [1–12], a phenomenological model based on the drift-diffusion model, the continuity equation for current, Poisson equation, and interband Zener tunneling process has been proposed to describe the transport processes in the oxide heterojunctions [13–16]. On the basis of this model, the transport mechanisms of the perovskite oxide heterojunctions at both forward and reverse bias voltages have been explained, respectively. However, the physical origin of the symmetric *I-V* curves, which have been commonly observed in the heterostructures of perovskite oxide at low temperatures, remains unrevealed [10,11]. Thus, a further understanding on the transport process in the oxide heterostructures is urgently considered.

In the perovskite heterostructures, a Schottky diode is formed easily at the interface of the perovskite oxide layer and the metal electrode due to the complicated interface states of the perovskite oxide material [17,18]. Thus, the *I–V* characteristics of an oxide heterostructures are not only determined by the p–n junction but also affected by the Schottky junction formed at the contact of the oxide layer and the metal electrode. In addition, with the temperature below the Curie temperature T_c of manganite, the transport property of the heterostructures of manganite/n-type (or p-type) oxide is determined not only by the Schottky junction formed at the interface of the metallic manganite and the n-type (or p-type) oxide but also by that formed at the interface of the electrode and the oxide. Therefore, a quantitative analysis for the effect of Schottky contact electrode on the transport property in the oxide heterostructures is highly desired.

In this work, we present the numerical study on the transport processes in the heterostructures of metallic-$La_{0.7}Sr_{0.3}MnO_3$/n-$BiFeO_3$ (LSMO/BFO) and p-$La_{0.9}Sr_{0.1}MnO_3$/n-$SrNb_{0.01}Ti_{0.99}O_3$ (LSMO/SNTO) by taking into account the effect of Schottky junctions formed at the contact of the indium electrode, respectively. Based on the calculation for Poisson equation, the drift-diffusion formula, and the tunneling processes, the energy band structure, the *I–V* curves, and the distributions of carriers in the heterostructures of LSMO/BFO and LSMO/SNTO are obtained self-consistently at various temperatures [14,15]. By comparing with the experimental data, the double-Schottky structure composed of the Schottky diode at the contact of the metallic-manganite and that of the metal electrode are revealed as the physical origin for the symmetric *I–V* curves measured in the

* Corresponding author. Tel./fax: +86 10 82648099.
E-mail address: kjjin@aphy.iphy.ac.cn (K.-j. Jin).

0921-4526/$ - see front matter © 2008 Elsevier B.V. All rights reserved.
doi:10.1016/j.physb.2008.12.018

heterostructures formed by manganite and n-type (or p-type) oxide with temperature below T_c. It is also found that the Schottky barrier formed at the interface of SNTO layer and the indium electrode plays an important role on the transport process of LSMO/SNTO heterostructures with temperature above T_c, and the effect of Schottky barrier increases with increased temperature and decreases with the increased doping density in SNTO layer, respectively.

2. Theoretical model

Due to the electronic states localized at the interface of BFO/metal and at that of SNTO/metal, Schottky junctions are formed easily at the contact of BFO layer with the metal electrode and at that of SNTO layer with the electrode [6,17], respectively. Here, we consider only the Schottky junction formed at the contact of BFO layer with the indium electrode in the LSMO/BFO heterostructures, and that formed at the contact of SNTO layer with the indium electrode in the LSMO/SNTO heterostructures, respectively. In our work, the thickness of heavily doped BFO and SNTO layer are about several hundreds of nanometers, which are much thicker than the widths of space charge region. Thus, the heterostructures of manganite/oxide/indium can be treated as a manganite/oxide junction in series with a oxide/indium Schottky junction in this work.

In case of temperature T below the Curie temperature T_c for LSMO, the hole-doped LSMO is a metallic manganite material, and a Schottky junction is formed at the interface of metallic manganite and n-type oxide layer. The distributions of electrostatic potential and carrier densities for Schottky junction with a given bias voltage are obtained by solving the drift-diffusion formulas, the continuity equation for current, and Poisson equation self-consistently with Richardson current as the interface condition [19,20]. In the heavily doped Schottky junction, the Richardson current, the direct and thermally assisted tunneling current dominate the forward transport process, while the direct and thermally assisted tunneling current are the dominant transport mechanisms for the reverse one [6,19,20]. Thus, the forward (or reverse) current density of a Schottky junction J_F (or J_R) with a bias voltage V_b is written as

$$J_F = A^* T^2 \exp\left(-\frac{q\Phi_B}{k_B T}\right)\left[\exp\left(\frac{qV_b}{k_B T}\right) - 1\right] + q\int_{E_c}^{E_{top}} N(E)f(E)T(E)\,\mathrm{d}E \quad (1)$$

and

$$J_R = q\int_{E_c}^{E_{top}} N(E)f(E)T(E)\,\mathrm{d}E, \quad (2)$$

where A^* is the effective Richardson constants of electron, Φ_B represents the effective barrier height of the Schottky junction, E_{top} denotes the top of the Schottky barrier, and E_c is the bottom of the conduction band for semiconductor layer, respectively. In addition, q represents the electric charge, $N(E)$ is the density of states, $f(E) = 1/(1+\exp((E-E_f)/k_BT))$ is the Fermi distribution function with E_f being the Fermi level and k_B being Boltzmann's constant, respectively. The tunneling rate $T(E)$ is calculated with the formula $T(E) = (\hbar/\sqrt{2m_c^* E})\Im[\psi_E^*(x)(\mathrm{d}/\mathrm{d}x)\psi_E(x)]$, where, "$\Im$" denotes the imaginary part of a complex number, $\hbar$ represents the reduced Planck constant, m_c^* is the electron effective mass, and $\psi_E(x)$ denotes the wave function obtained by solving the Schrödinger equation [21], respectively.

With temperature above the T_c, the LSMO material behaves as a p-type semiconductor. Thus, a p–n junction is formed at the interface of p-manganite and n-oxide layer. The formulas, the boundary conditions, and the detailed arithmetic for solving the transport process of the perovskite oxide p–n junctions have been given in elsewhere [14,15,22,23]. With the method introduced in Refs. [14,22], the behaviors of electrostatic potential $\phi(x)$, electron concentration $n(x)$, hole concentration $p(x)$, and the I-V curves of the perovskite p–n junction under the external bias voltage are obtained self-consistently.

3. Results and discussion

In case of temperature below T_c, the heterostructures of manganite/oxide/indium is treated as a Schottky junction of manganite/oxide in series with a Schottky junction of oxide/indium. Thus, a symmetric double-Schottky structure is formed. The energy band of a double-Schottky structure with bias voltage is plotted in Fig. 1.

To study the transport process in the double-Schottky structure, we present our calculation on the heterostructures of $La_{0.7}Sr_{0.3}MnO_3/BiFeO_3$/indium (LSMO/BFO/In). The heterostructures of LSMO/BFO/In was fabricated on $SrTiO_3$ substrate with indium as the top electrode on the surface of BFO and the metallic LSMO as the bottom electrode [24], respectively. Due to the high Curie temperature of $La_{0.7}Sr_{0.3}MnO_3$ [25], the $La_{0.7}Sr_{0.3}MnO_3$ material behaves as a metallic manganite with temperature between 200 and 270 K. As a result, the heterostructures of LSMO/BFO/In can be modeled as a double-Schottky structure at that temperature range. The comparisons between the calculated and the measured I-V curves of LSMO/BFO/In heterostructures with various temperatures are given in Fig. 2. In the calculation, the concentration of donor in BFO $N_d = 2.0\times10^{19}\,\mathrm{cm}^{-3}$, the height of Schottky barrier is taken as 0.65 eV, while the band gap of BFO is 2.8 eV [26], other necessary parameters used in the calculation are taken from Ref. [27]. As shown in Fig. 2, the experimental data obtained from our previous work [28] are denoted by hollow squares, circuits, triangles, and stars with temperature as 200, 230, 250, and 270 K, respectively, while the solid, dotted, dashed, and dotted dashed curves represent the theoretical I–V curves at $T = 200, 230, 250$, and 270 K, respectively. Comparing the experimental and calculated data, it is found that the symmetric I–V curves observed in the heterostructures of metallic-manganite/n-type (or p-type) oxide is caused by the double-Schottky structure. In addition, the physical origin for

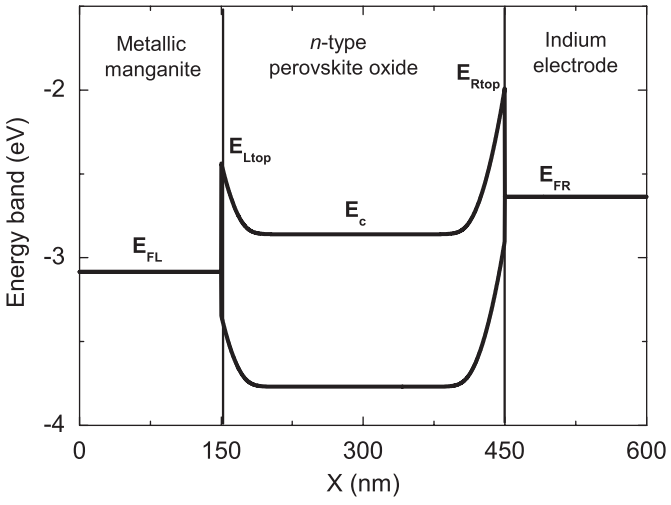

Fig. 1. The band-energy diagrams of the $La_{0.7}Sr_{0.3}MnO_3/BiFeO_3$/indium double-Schottky structure with a given bias voltage.

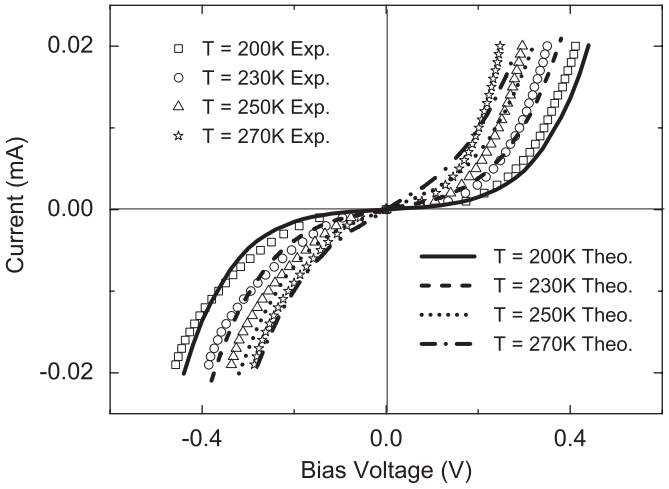

Fig. 2. The comparison between theoretical and experimental *I–V* curves of LSMO/BFO/In heterostructures at various temperatures. The hollow squares (or solid curve), the hollow circuit (or dashed curve), the hollow triangle (or dotted curve), and the hollow stars (or dashed and dotted curves) represent the experimental (or theoretical) *I–V* curves at $T = 200, 230, 250$, and 270 K, respectively.

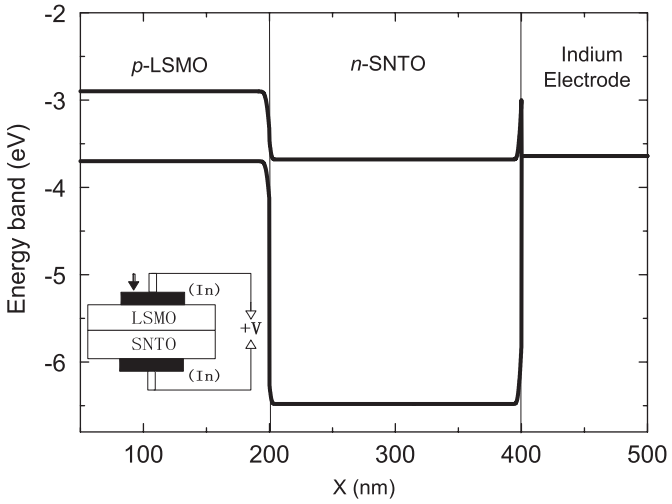

Fig. 3. The band-energy profile of the $La_{0.9}Sr_{0.1}MnO_3/SrNb_{0.01}Ti_{0.99}O_3$/indium heterostructures without bias voltage.

the symmetric *I-V* curves observed in the manganite/titanate heterostructures at low temperature [10,11] can be attributed to the double-Schottky structure formed by the Schottky contact diodes.

For the 10% Sr doped $LaMnO_3$, the T_c is below 150 K [25]. Thus, the theoretical *I-V* curves of $La_{0.9}Sr_{0.1}MO_3/SrNb_{0.01}Ti_{0.99}O_3$/indium (LSMO/SNTO/In) heterostructures are calculated by treating this heterostructures as a LSMO/SNTO p–n junction in series with a SNTO/In Schottky junction at temperature between 200 and 300 K. The calculated energy band profile of the LSMO/SNTO/In heterostructures without bias voltage is given in Fig. 3. The theoretical *I–V* curves at $T = 200, 250$, and 300 K with forward bias on the LSMO/SNTO/In heterostructures are plotted in Fig. 4(a), (b), and (c), respectively. In these figures, the dashed curves represent the *I-V* curves of SNTO/In Schottky junction, the dotted curves denote those of LSMO/SNTO p–n junction, and the solid curves are the total *I–V* curves of the LSMO/SNTO/In heterostructures, respectively. In the calculation, the height of Schottky barrier is taken as 1.2 eV [17], while the concentrations of the acceptor and the donor are $N_a = 4.0 \times 10^{19}\,cm^{-3}$ and $N_d = 6.0 \times 10^{20}\,cm^{-3}$, respectively. The other necessary parameters for our calculation are taken from Refs. [13,15], respectively. As shown in Fig. 4(a)–(c), the resistance of p–n junction is greater than that of Schottky junction and decreases with the increased temperature at the temperature range of 200–300 K. According to the principle of series circuit, the *I–V* characteristics of the LSMO/SNTO/In heterostructures are mainly determined by the transport property of the LSMO/SNTO p–n junction, and the Schottky contact electrode also plays an important role in the transport process. Furthermore, the contribution of LSMO/SNTO p–n junction on the *I–V* characteristics of LSMO/SNTO/In heterostructures decreases and that of the Schottky barrier increases with increased temperature, respectively.

To investigate the effect of Schottky contact electrode on the transport properties of LSMO/SNTO/In heterostructures with various doping densities in SNTO layer, we calculate the *I–V* curves of the LSMO/SNTO p–n junction, the SNTO/In Schottky junction, and the LSMO/SNTO/In heterostructures with $N_d = 4.0 \times 10^{20}\,cm^{-3}$, $5.0 \times 10^{20}\,cm^{-3}$, and $6.0 \times 10^{20}\,cm^{-3}$ at $T = 300$ K, respectively. The comparisons between the *I–V* curves with various doping densities are given in Fig. 5(a)–(c). As plotted in

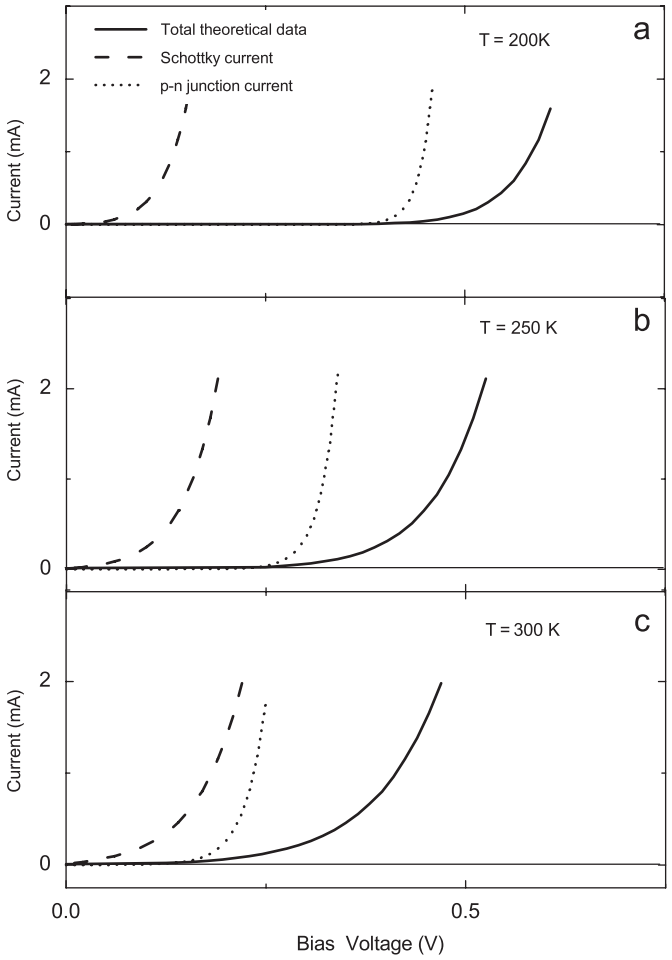

Fig. 4. The calculated *I–V* curves of LSMO/SNTO/In heterostructure at (a) $T = 200$ K, (b) $T = 250$ K, and (c) $T = 300$ K, respectively. In this figure, the solid, dashed, and dotted curves represent the calculated *I–V* characteristics of the LSMO/SNTO/In heterostructure, the SNTO/In Schottky junction, and the LSMO/SNTO p–n junction, respectively.

these figures, the resistance of Schottky junction increases with the decrease in N_d due to the increased barrier width for the Schottky junction. Thus, the effect of Schottky barrier on the

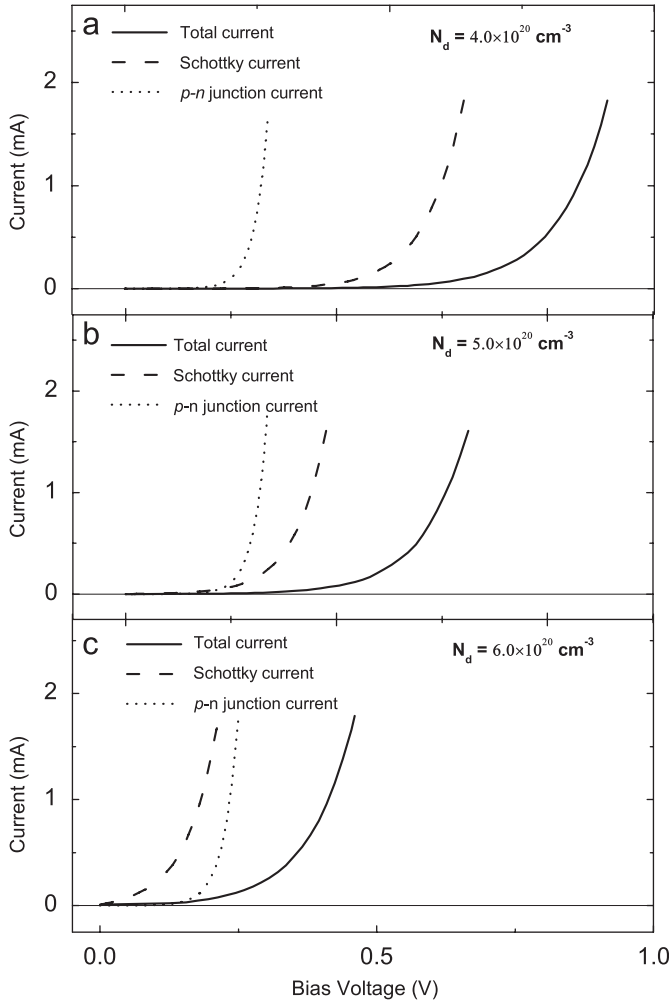

Fig. 5. The comparison between calculated I–V curves of LSMO/SNTO/In heterostructures at $T = 300$ K with (a) $N_d = 4.0 \times 10^{20}$ cm^{-3}, (b) $N_d = 5.0 \times 10^{20}$ cm^{-3}, (c) $N_d = 6.0 \times 10^{20}$ cm^{-3}, respectively. In this figure, the solid, dashed, and dotted curves represent the calculated I–V characteristics of the LSMO/SNTO/In heterostructure, the SNTO/In Schottky junction, and the LSMO/SNTO p–n junction, respectively.

transport property of LSMO/SNTO/In heterostructures increases with the decreased doping density of the SNTO layer.

With an applied reverse bias on the LSMO/SNTO/In heterostructures, a reverse bias voltage is on the LSMO/SNTO p–n junction and a forward bias voltage is on the SNTO/In Schottky junction, respectively. Because the resistance of LSMO/SNTO p–n junction with reverse bias is much greater than that of the SNTO/In Schottky junction with forward bias, the I-V characteristics of the LSMO/SNTO/In heterostructures under reverse bias are dominated by the transport properties of the LSMO/SNTO p–n junction. It should be pointed out that the interband and trap assisted tunneling processes have been revealed as the dominant transport mechanisms for the LSMO/SNTO p–n junction under reverse bias in our previous work [15,29].

4. Summary

In summary, the effect of Schottky barrier formed at the contact of electrode on the transport properties of perovskite oxide heterostructures has been studied theoretically. The results obtained in our work reveal that the physical origin for the symmetric I–V curves observed in the heterostructures formed by manganite and n-type (or p-type) oxide with temperature below T_c can be attributed to the double-Schottky structure. It is also found that the influence of Schottky junction formed at the interface of electrode and oxide on the I–V characteristics of manganite/oxide/indium heterostructures increases with increased temperature and decreases with the increased doping density in oxide layer at temperature above T_c.

Acknowledgments

This work was supported by the National Natural Science Foundation of China, and the National Basic Research Program of China.

References

[1] M. Sugiura, K. Uragou, M. Tachiki, T. Kobayashi, J. Appl. Phys. 90 (2001) 187.
[2] H. Tanaka, J. Zhang, K. Kawai, Phys. Rev. Lett. 88 (2002) 027204.
[3] J. Zhang, H. Tanaka, T. Kawai, Appl. Phys. Lett. 80 (2002) 4378.
[4] H.B. Lu, G.Z. Yang, Z.H. Chen, S.Y. Dai, Y.L. Zhou, K.J. Jin, B.L. Cheng, M. He, L.F. Liu, H.Z. Guo, Y.Y. Fei, W.F. Xiang, L. Yan, Appl. Phys. Lett. 84 (2004) 5007.
[5] H.B. Lu, S.Y. Dai, Z.H. Chen, Y.L. Zhou, B.L. Cheng, K.J. Jin, L.F. Liu, G.Z. Yang, X.L. Ma, Appl. Phys. Lett. 86 (2005) 032502.
[6] T. Susaki, N. Nakagawa, H.Y. Hwang, Phys. Rev. B 75 (2007) 104409.
[7] A. Ruotolo, C.Y. Lam, W.F. Cheng, K.H. Wong, C.W. Leung, Phys. Rev. B 76 (2007) 075122.
[8] C. Mitra, P. Raychaudhuri, G. Köbernik, K. Dörr, K.H. Müller, L. Schultz, R. Pinto, Appl. Phys. Lett. 79 (2001) 2408.
[9] C. Mitra, P. Raychaudhuri, K. Dörr, K.H. Müller, L. Schultz, P.M. Oppeneer, S. Wirth, Phys. Rev. Lett. 90 (2003) 017202.
[10] Z.G. Sheng, W.H. Song, Y.P. Sun, J.R. Sun, B.G. Shen, Appl. Phys. Lett. 87 (2005) 032501.
[11] H.B. Lu, S.Y. Dai, Z.H. Chen, L.F. Liu, H.Z. Guo, W.F. Xiang, Y.Y. Fei, M. He, Y.L. Zhou, G.Z. Yang, Chinese Phys. Lett. 20 (2003) 137.
[12] F.Y. Bruno, J. Garcia-Barriocanal, M. Torija, A. Rivera, Z. Sefrioui, C. Leighton, C. Leon, J. Santamaria, Appl. Phys. Lett. 92 (2008) 082106.
[13] K.-j. Jin, H.B. Lu, Q.L. Zhou, K. Zhao, B.L. Cheng, Z.H. Chen, Y.L. Zhou, G.Z. Yang, Phys. Rev. B 71 (2005) 184428.
[14] Q.L. Zhou, K.-j. Jin, H.B. Lu, P. Han, Z.H. Chen, K. Zhao, Y.L. Zhou, G.Z. Yang, Europhys. Lett. 71 (2005) 283.
[15] P. Han, K.-j. Jin, H.B. Lu, Q.L. Zhou, Y.L. Zhou, G.Z. Yang, Appl. Phys. Lett. 91 (2007) 182102.
[16] C.L. Hu, P. Han, K.-j. Jin, H.B. Lu, G.Z. Yang, J. Appl. Phys. 103 (2008) 053701.
[17] M. Minohara, I. Ohkubo, H. Kumigashira, M. Oshima, Appl. Phys. Lett. 90 (2007) 132123.
[18] N. Nakagawa, M. Asai, Y. Mukunoki, T. Susaki, H.Y. Hwang, Appl. Phys. Lett. 86 (2005) 082504.
[19] S.F. Guo, Solid-State Electron. 27 (1984) 537.
[20] R.B. Darling, Solid-State Electron. 31 (1988) 1031.
[21] O. Pinaud, J. Appl. Phys. 92 (2002) 1987.
[22] K. Horio, H. Yanai, IEEE Trans. Electron. Devices 37 (1990) 1093.
[23] P. Han, K-j. Jin, Y. Zhou, X. Wang, Z. Ma, S.F. Ren, A.G. Mal'shukov, K.A. Chao, J. Appl. Phys. 99 (2006) 074504.
[24] G.Z. Liu, C. Wang, C.C. Wang, J. Qiu, M. He, J. Xing, K.-j. Jin, H.B. Lu, G.Z. Yang, Appl. Phys. Lett. 92 (2008) 122903.
[25] E. Dagotto, T. Hotta, A. Moreo, Phys. Rep. 344 (2001) 1.
[26] S.J. Clark, J. Robertson, Appl. Phys. Lett. 90 (2007) 132903.
[27] H. Yang, M. Jain, N.A. Suvorova, H. Zhou, H.M. Luo, D.M. Feldmann, P.C. Dowden, R.F. DePaula, S.R. Foltyn, Q.X. Jia, Appl. Phys. Lett. 91 (2007) 072911.
[28] J. Qiu, H.B. Lu, M. He, G.Z. Liu, K.-j. Jin, Phys. B, under review.
[29] P. Han, J.F. Jia, Phys. Lett. A 372 (2008) 4943.